PNAS RESEARCH ARTICLE | ENVIRONMENTAL SCIENCES

Logging disrupts the ecology of molecules in headwater streams

Erika C. Freeman[a,b,1], Erik J. S. Emilson[c,d], Kara L. Webster[c], Thorsten Dittmar[e,f], and Andrew J. Tanentzap[a,d,e]

Affiliations are included on p. 9.

Edited by Donald Canfield, Syddansk Universitet, Odense M, Denmark; received May 9, 2024; accepted July 22, 2025

Global demand for wood products is increasing forest harvest. One understudied consequence of logging is that it accelerates mobilization of dissolved organic matter (DOM) from soils to aquatic ecosystems where it is more easily rereleased to the atmosphere. Here, we tested how logging changed DOM in headwaters of hardwood-dominated catchments in northern Ontario, Canada. We applied a before-after-control-impact experiment across four catchments for 3 y and measured DOM monthly during ice-free seasons. DOM concentration in streams from logged catchments quadrupled, on average, only for the first 2 mo postharvest, but resulting changes to the molecular composition of DOM persisted for at least 2 y. Ultrahigh-resolution mass spectrometry revealed that DOM composition within logged streams became more available for microbial use and chemically diverse than in controls, with novel highly unsaturated polyphenols, carboxylic-rich alicyclic, and nitrogen-containing formulae. The molecular composition of stream DOM measured fortnightly postharvest was most similar to the DOM composition of surrounding soils, likely due to increased hydrological connectivity. Alongside carbon being more likely to be released into the atmosphere, we estimate that selective logging increased the total flux of dissolved organic carbon in streams by 6.4% of the carbon extracted as timber. Although these estimates are short-lived, they should affect the millions of hectares that are logged annually. Carbon accounting of forestry, including as a natural climate solution, must now consider the transport and fate of DOM from land into water.

dissolved organic matter | streams | logging

Significance

Logging is widespread and growing in frequency, partly to increase terrestrial carbon sequestration. However, logging can change the amount and reactivity of stable soil organic matter that becomes dissolved in water, thereby offsetting some of its efficacy as a natural climate solution. Using a paired-catchment experiment, we observed a short-lived increase in concentrations of stream carbon but persistent shift in its molecular composition toward greater reactivity after logging. We estimated that these changes to dissolved organic matter pools were large enough to switch logging from a carbon-sink to carbon-neutral or even carbon-source. Our work revises downward potential carbon sequestration in wood products from hemi(boreal) forests and suggests that best management practices can be improved to make logging sequester more carbon.

Long-lasting wood products and subsequent forest regrowth generated from logging are increasingly used as natural climate solutions to sequester atmospheric carbon (1, 2). However, logging inherently disturbs the ability of forests to sequester carbon, potentially offsetting the very benefits it aims to achieve. One disturbance caused by logging involves changing carbon export from soils into receiving waters. In northern Sweden, logging practices were found to mobilize 8 to 18% of annual terrestrial net ecosystem productivity from soils into headwater streams as dissolved organic matter (DOM), partly because the loss of tree cover enhanced soil wetness and expanded saturated areas (3). Similar increases in DOM export have been found in other boreal forests (4), but ref. 5 reported no change, and decreases have been reported in some temperate (6) and tropical systems (7). Despite the potentially large flux, the amount of terrestrial carbon lost downstream during logging versus that stored in harvested biomass is rarely measured and often assumed negligible. Once released as DOM into headwaters by logging, terrestrial carbon may be more likely to be respired back to the atmosphere than in unimpacted streams or had it remained as mineral-associated organic matter in soils (8). The likelihood of terrestrial carbon returning to the atmosphere ultimately depends on the composition of DOM entering headwaters. Forest harvesting activities can change DOM composition by increasing overland and near surface lateral flow, physically disturbing soils with heavy machinery, and generating woody debris (9–11). Compared with soils, especially mineral-associated organic matter, DOM is also far more reactive because it is readily available for microbial metabolism (12, 13). Quantifying the amount and composition of carbon exported from soils into waters after logging is now needed to estimate accurately the efficacy of natural climate change solutions and design more effective forest management practices.

Once logging-displaced carbon enters waterways, its fate as a carbon source or sink will partly depend on the interactions among the thousands of different compounds within DOM. Each compound in a DOM mixture has unique intrinsic properties that influence how it interacts with other compounds and physicochemical and biological processes (14). These interactions—termed the "ecology of molecules" (14, 15)—can be measured from the presence of unique molecular formulae in a mixture (termed "chemodiversity") and the proportion of different compound classes, typically identified based on elemental ratios of

Author contributions: E.C.F., E.J.S.E., and A.J.T. designed research; E.C.F. performed research; E.J.S.E. and T.D. contributed new reagents/analytic tools; E.C.F. analyzed data; and E.C.F., E.J.S.E., K.L.W., T.D., and A.J.T. wrote the paper.

The authors declare no competing interest.

This article is a PNAS Direct Submission.

[1]To whom correspondence may be addressed. Email: erika.freem@gmail.com.

This article contains supporting information online at https://www.pnas.org/lookup/suppl/doi:10.1073/pnas.2409104122/-/DCSupplemental.

Published August 26, 2025.

individual formulae (16). Both chemodiversity and compound composition influence microbial metabolic efficiency and physicochemical reactivity (16, 17) and thus the likelihood of compounds being respired to the atmosphere (18). For example, carboxylic-rich alicyclic molecules (CRAMs) containing relatively intermediate H:C and O:C ratios tend to be less reactive, and so may persist longer in the environment (19, 20), whereas high H:C (>1.5) nonaromatic and high N and P-containing formulae (21–23) are preferentially degraded by microbes and so may be more easily respired (24, 25). Advances in ultrahigh-resolution mass spectroscopy (UHR-MS) now provide an opportunity to characterize the ecology of molecules and its implications for forest carbon budgets.

Here, we report how logging changes the quantity and molecular composition of DOM in headwater streams to reflect surrounding hillslope soils. Headwater streams are where forest runoff is first channeled into downstream waters and collectively account for most of the stream length on Earth (26). Because temperate forests are major timber producers and are expected to face increasing harvest pressure under climate change (27), we undertook an experiment in four hardwood-dominated headwater catchments in Canada. Two catchments were selectively harvested, each with paired unharvested controls with nearly identical climate, underlying geology, size, and topography (*Materials and Methods*). We quantified spatial and temporal differences in DOM molecular composition before and after forest harvest over 3 y using an asymmetrical before-after-control-impact (BACI) statistical design. Water was collected monthly during the ice-free season both from the channel heads of streams within each catchment and from soil porewaters at multiple depths along hillslopes. We measured DOM composition with complementary analytical chemistry approaches, namely Fourier-transform ion cyclotron resonance mass spectrometry (FT-ICR MS) and optical spectroscopy. Although optical properties cannot resolve the ecology of molecules, they are easier to measure at high temporal resolution than individual molecular formulae, and so can serve as a useful indicator of changes in chemodiversity and compound classes (28). We then tested how DOM concentration and composition changed across the period immediately before and after logging (i.e., 2020) and the entire study period (i.e., 2019 to 2021) to separate both short- and long-term impacts of logging. By replicating catchments and sampling repeatedly through time, our asymmetrical BACI design was particularly powerful for detecting pulse responses to disturbances and changes to temporal variability alongside mean effects (29). Overall, we report large changes in DOM composition that will ultimately influence the efficacy of wood products as a nature-based climate solution, and we identify the sources of these changes in upland soils to improve forest management aimed at climate change mitigation.

Results

The Immediate Mobilization of DOM after Forest Harvest. Consistent with past evidence that forest harvest increases DOM export to streams (3), we found DOM concentrations were temporarily elevated in the logged catchments relative to the controls in 2020, the year of harvest (Fig. 1 and *SI Appendix*, Table S1). Because we modeled the effect of time on DOM concentrations as a continuous variable, we could identify that differences in concentrations were largest between 2 mo (i.e., by the end of 2020) and 7 mo (i.e., by spring 2021) after harvest within the longer 3-y study period (Fig. 1 and *SI Appendix*, Table S1). The sampling frequency, particularly immediately postlogging, may influence precise peak identification; the observed peak is the largest captured by our design. This short-term selective forest harvest (*Materials and Methods*) largely offset the decline in DOM seen in the controls after increased seasonal discharge (30, 31) (Fig. 1*B* and *SI Appendix*, Fig. S1). The estimated rate of change in DOM concentrations observed in the harvested streams (0.08 mg C L^{-1} d^{-1}; SE: ± 0.31 mg C L^{-1} d^{-1}, $P = 0.023$) was large enough that the mean concentration increased by 100% from initial values (1.22 ± 0.38 mg C L^{-1} d^{-1}) and by 600% relative to the controls by the end of the growing season (Fig. 1*B*). Cation and heavy metal concentrations increased similarly in the streams of the harvest sites, indicative of increased nutrient leaching from disturbed soils (4) (*SI Appendix*, Table S2). These elevated DOM concentrations returned to baseline levels by 2021 (*SI Appendix*, Table S3).

To compare the stream DOM fluxes with estimates of carbon removed as wood biomass by logging, we estimated carbon export in runoff associated with harvesting. We multiplied the modeled difference in DOM concentrations between the harvest and control catchments from October-November 2020 by the corresponding monthly runoff averaged in 9 similarly sized local catchments (*Materials and Methods*). The values were then converted to areal units based on catchment size. We estimated that the harvested sites exported an additional 13 kg C mo^{-1} ha^{-1} (SE: ± 4 kg C mo^{-1} ha^{-1}) of DOM compared to the nonharvested catchments. If this increase remained constant for the first year postharvest (n = 8 nonwinter months), an additional ca. 6.4% of the carbon that was harvested as above-ground woody biomass would be lost to the streams solely through increased DOM export (*Materials and Methods*). While our estimate represents the maximum effect of forest harvesting on DOM export in a single logging event, others have found these effects to persist for months to years (3). We also assume that differences between harvest and control catchments disappear by the next growing season consistent with our 2021 observations (Fig. 1*B*). Although seemingly small, the 6.4% of woody biomass that we found was lost to downstream waters is large enough to switch logging from a carbon sink to carbon neutral or even carbon source. Recent estimates indicate that wood products from (hemi)boreal forests store a net of 22 Tg C y^{-1}, when multiplying global transfer from forests into wood products (32, 33) by the amount of wood production in majority (hemi) boreal countries (Canada, Russia, Sweden, Finland, Norway, Lithuania, Latvia, and Estonia) (FAO, 2023). As DOM losses to waterways are generally excluded from forest carbon accounting, we estimated that logging-induced DOM export would cause an additional 16 Tg C y^{-1} loss across (hemi)boreal forests. We derived this number by multiplying the loss of DOM (6.4%) by the product of the gross amount of carbon lost globally from harvest activities (1,040 Tg C y^{-1}; 34–36) and contribution of (hemi)boreal countries (24.1%) to global harvest activities. This unaccounted pathway would reduce net (hemi)boreal wood product storage to 6 Tg C y^{-1}, demonstrating that current estimates may overstate forestry's climate benefits in northern regions. The net change in carbon may even be negative if best management practices (BMPs) are not applied or downstream losses of carbon are larger than reported here, e.g., ref. 37. For example, a meta-analysis incorporating data from multiple studies with similar soil type and identical forest harvesting practices to our study indicates that logging reduces soil C by a mean 11.2% (SE: ± 5.7%, n = 945) (38). More broadly, our study illustrates how accounting for aquatic losses of soil carbon in monitoring and modelling has a major impact on forest policy and climate change mitigation strategies.

Changes to DOM Composition Persist after Forest Harvest. Our results suggest that while there is an increase in DOM concentration only in the first 2 mo after harvest, which subsequently returns to predisturbance levels (Fig. 1*B* and *SI Appendix*, Tables S1–S3), the

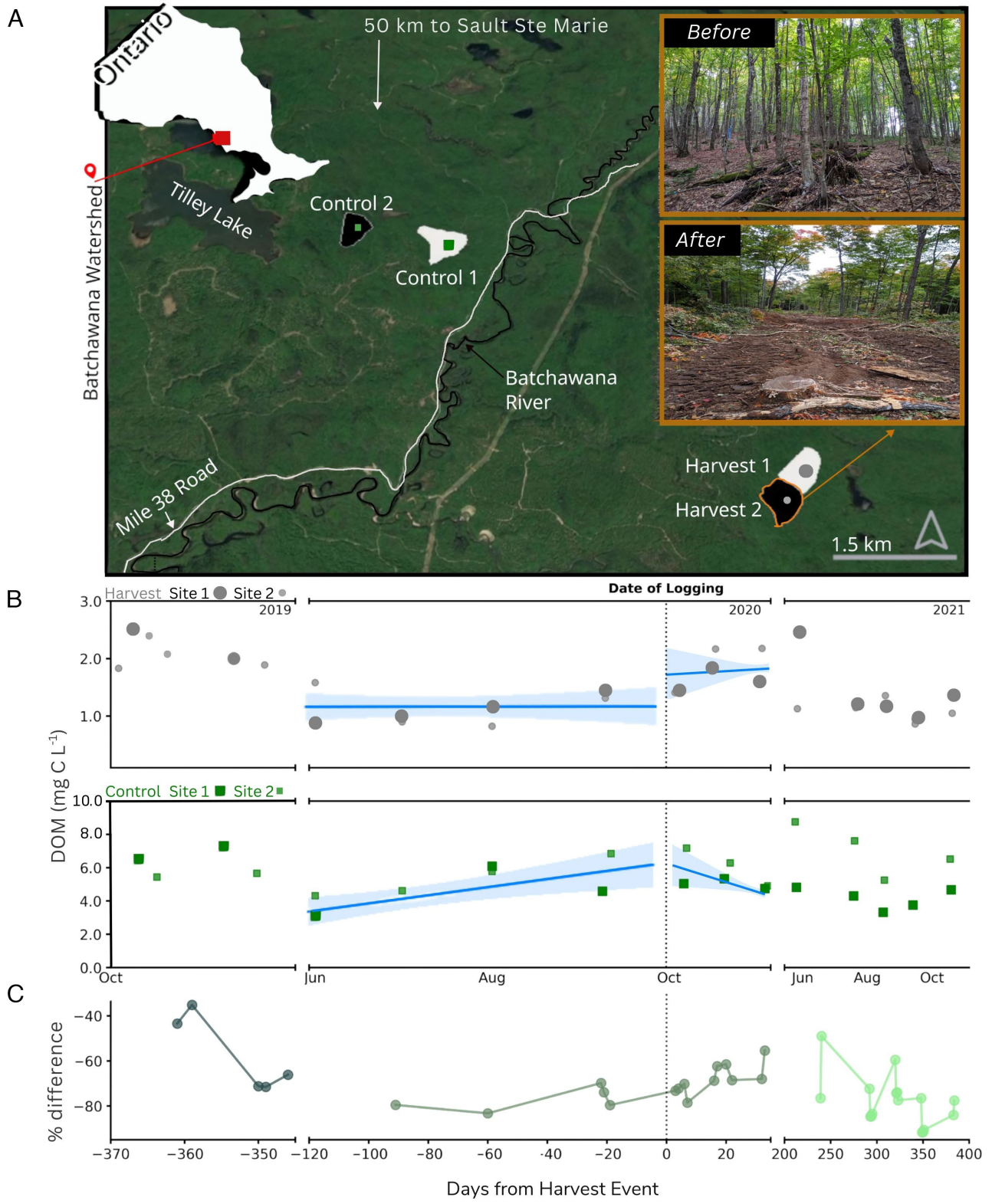

Fig. 1. DOM concentrations were elevated in streams of the harvest relative to the control sites immediately after logging. (*A*) Map of experimental catchments within the Batchewana Watershed, ON, Canada. The four replicate catchments were named based on the impact classification. Control sites were unharvested, and logged sites were logged in late September 2020 (bolded dashed line in *Bottom* panel). Sites with the same symbol emphasis (bold or light) indicate a control-harvest pair based on climate, geology, and catchment size and topology. (*B*) DOM concentrations faceted by year (2019, 2020, and 2021) and treatment (logged upper, control lower). Estimated mean ± 95% CI for temporal trends were plotted as blue lines ± bands where there were statistically significant differences between treatments (*SI Appendix*, Table S1). (*C*) The difference harvest control for the paired catchments relative to the control (additional DOM metrics in *SI Appendix*, Figs. S8 and S9).

molecular composition of DOM in streams remained influenced by forest harvest well after the initial DOM pulse (*SI Appendix*, Figs. S7 and S8 and Table S3). We initially characterized the mean or bulk character of DOM using optical properties because we could measure these at high temporal resolution, i.e., monthly for 3 y during the ice-free season (39). We found that the humification

index (HIX), which is a unitless measure of the complexity of DOM, increased by 62.5% from a mean of 5.17 (SE: 2.73) before the harvest to 8.40 (SE: 3.83) within 2 mo after harvest (P = 0.034, *SI Appendix*, Table S2). This result indicated that DOM was becoming more polycondensed (lower H:C ratio), or, more soil-like (40). The increase in HIX was a mean 4.56 (SE: 1.75) larger than in the controls between 2019 and 2021 (P = 0.041). In contrast to the increase postharvest, HIX declined between 2019 and 2021 by a mean of 30.1% in the control catchments (SE: 7.2) from a mean of 18.37 (SE: 2.22) to 12.83 (SE: 2.27; P = 0.007), indicating long-term leaching of soil DOM only into the harvested streams (*SI Appendix*, Fig. S1). None of the other optical properties varied with logging (*SI Appendix*, Figs. S7 and S8 and Table S3).

To identify changes in DOM composition, we associated the optical properties with UHR-MS. We detected 7,444 distinct molecular formulae across all streams using FT-ICR MS of solid-phase extractable DOM collected monthly during the ice-free season in 2020. A fraction of these molecular formulae (13% and 16%) were positively and negatively correlated with HIX, respectively (Fig. 2*A*). Although there are uncertainties in analyzing the intensities of molecular formulae, these are proportional to concentrations for individual molecules (41) and so can be used to identify trends in each molecule using rank-based correlations. We correlated commonly used descriptive traits of molecular formulae to the strength of the correlation between the relative intensity of each formula and the HIX value of the corresponding DOM pool across all sampling dates in 2020. We found that molecular formulae that were more positively associated with HIX had larger values of the formula-based estimate of aromaticity (Fig. 2*B*; AI_{mod}, ρ = 0.62, P < 0.001), which indicates the presence of condensed aromatic structures (42). The association with AI_{mod} was stronger than with any other metric (Fig. 2*B*). This result confirms that stream DOM was becoming more like surface soil postlogging and was confirmed by leaching studies performed at the site (43). Studies in lake sediment have found that AI_{mod} strongly correlates with the relative abundance of aromatic highly unsaturated compounds (44), further supporting a terrestrial origin to the HIX signal rather than changes produced in-stream (45, 46). While our results indicate that logging transported terrestrial-like compounds downstream, the fate of these compounds is less clear. Most of the compounds that correlated with HIX in our study had H:C < 1.1 (Fig. 2*A*) and AI_{mod} > 0.25 (*SI Appendix*, Fig. S1), suggesting that the compounds added to streams postlogging may be more reactive than those in prelogging conditions.

We found that logging substantially increased the potential for soil carbon to be processed downstream by microbes compared with natural temporal variation observed in control streams. We first calculated the potential energy released by each molecular formula based on the Gibbs free energy (GFE) associated with the oxidation of carbon (47, 48). Compounds with a higher GFE yield less energy and so are preferentially respired rather than used to construct biomass (47). Although we found that GFE differed by only a mean of 6% between control and harvest streams before logging, its decline in harvest streams after logging was four times greater than in the controls (*SI Appendix*, Fig. S2 and Table S4, P = 0.024), indicating that the compounds added to streams were relatively more likely to be respired (47). Compounds in the harvested streams were also predicted to undergo greater microbial processing after logging. We calculated the potential number of biochemical transformations that each molecule could undergo, which depends on how compounds react with each other in the environment. Transformations are only considered to be present if both end-members of a known reaction are present (49–51). Our analysis revealed a statistically significant difference in the number of transformations between sampling periods (before and after logging) between harvest and control streams (P = 0.043, *SI Appendix*, Fig S3 and Table S5). There was a mean 52% (SE: 33%) increase in the number of transformations that each formula could undertake in logged streams after forest harvest versus the controls (*SI Appendix*, Fig. S3 and Table S5). Together, these results indicate that the changes in the molecular composition of DOM after logging are likely to increase outgassing and further reduce the carbon sink capacity of forestry.

The Terrestrial Source of Increasing Stream Chemodiversity. We expected that forest harvest would reduce chemodiversity in streams as DOM became homogenized by high soil hydrological connectivity induced by harvest (52). However, we found a 32% increase in the number of unique compounds after forest harvest compared to the controls (Fig. 3*A*). The number of unique compounds increased from a mean of 4,771 (SE: 330 compounds) to 6,292 (SE: 390 compounds, P = 0.020), whereas compounds declined in controls from a mean of 5,387 (SE:

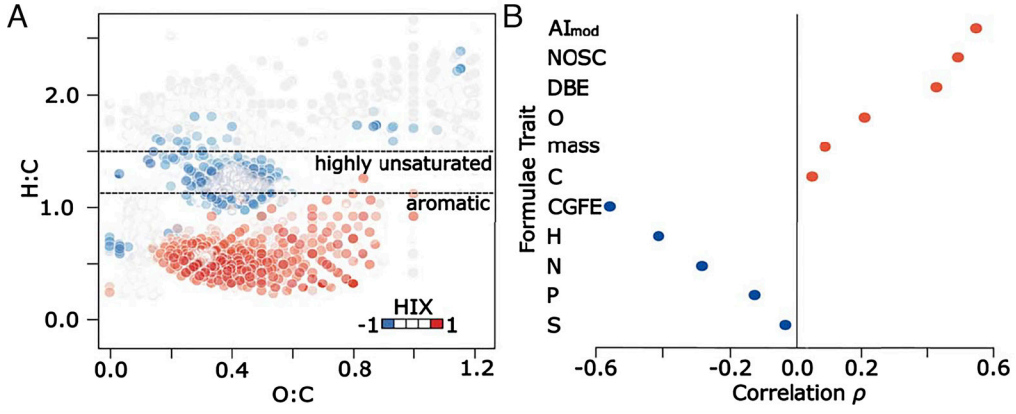

Fig. 2. Forest harvest led to persistent increases in the HIX of DOM in headwater streams. (*A*) Elemental ratios of all molecular formulae detected in our experiment (n = 7,444). Red and blue points are formulae whose relative peak intensities correlate (P < 0.05) positively and negatively with HIX, respectively, based on Spearman rank correlations. Dotted lines indicate aromatic compounds (H:C < 1.1) and the "highly unsaturated" region (1.1 < H:C < 1.5) according to ref. 43. (*B*) Spearman rank correlation (ρ) between either the modified aromaticity index (AI_{mod}), NOSC, DBE, number of oxygen atoms (O), molecular mass, number of carbon (*C*) atoms, GFE, and the number of hydrogen (H), nitrogen (N), phosphorus (P), and sulfur (S) atoms of each molecular formula against the correlation between the relative abundance of each molecular formulae and the HIX of the corresponding DOM pool across all time points (n = 7) measured in 2020 with UHR-MS. For all correlations, P < 0.05.

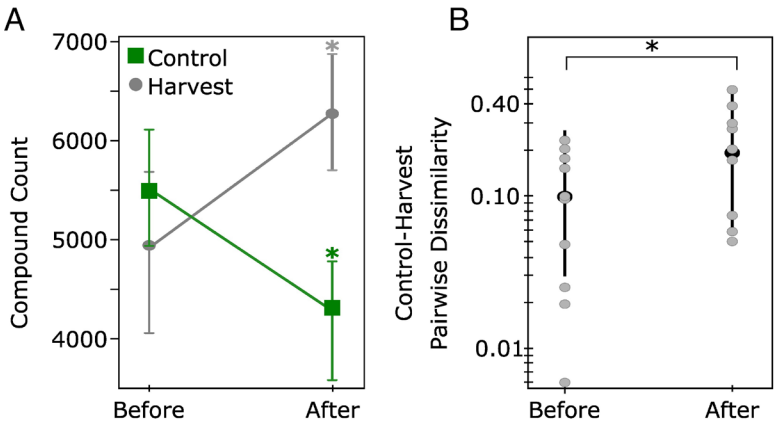

Fig. 3. Forest harvest increases molecular diversity of DOM in headwater streams. (*A*) Estimated mean (±95% CI) compound counts in streams draining control and harvested forests before and after logging. The green and gray asterisks indicate statistically significant differences based on a mixed effects model ($P < 0.05$) between control and harvest after logging, and before and after forest logging, respectively (*SI Appendix*, Table S6). (*B*) Estimated mean (±95% CI) pairwise dissimilarity (log-scale) between paired control and harvest sites both before and after logging (*SI Appendix*, Table S7). Gray points are individual observations at each time point based on the Bray–Curtis dissimilarity (*SI Appendix*, Fig. S5). The asterisk indicates a statistically significant difference ($P < 0.05$) between the mean pairwise dissimilarity before and after logging using a mixed effects model.

399 compounds) to 4,153 (SE: 260 compounds, $P = 0.013$, *SI Appendix*, Table S6). This decline in the controls corresponded with seasonal reductions in runoff observed across all three study years (*SI Appendix*, Fig. S4). We found further support for a diversification of DOM postlogging using a multivariate analysis of its molecular composition. We calculated the Bray–Curtis dissimilarity between control and harvest sites at each time point. The pairwise distance between paired sites increased after harvest (Fig. 3*B*), suggesting that the molecular composition of DOM was increasingly differentiated. Furthermore, the harvest sites differed more between the before and after samples than the controls (Fig. 3). While an ordination reveals some differences in the molecular composition of control and harvest catchments prior to logging, the magnitude of these differences was relatively small (*SI Appendix*, Fig. S5). Before disturbance, the mean difference in molecular composition between control and harvest sites was 10%, with half of the differences <5% (Fig. 3*B*). In contrast, composition diverged between treatments much more strongly postlogging with a mean dissimilarity of 20% and half of the differences >30% (Fig. 3*B*, $P = 0.003$). These results are a direct report that DOM becomes more diverse after forest harvest (*SI Appendix*, Table S7) and contrast our expectations based on observations from stream networks that the molecular composition of DOM should become homogenized (52).

We explored the mechanism underlying the unexpected increase in chemodiversity by analyzing the compounds that were gained in the logged sites after forest harvest. Generally, vascular plant-derived DOM is aromatic and has a low H:C and high O:C ratio (53, 54). Consistent with this interpretation, we found that the compounds gained after logging had higher O:C ratios (Fig. 4 *A* and *C*). There was also a greater proportion of highly unsaturated phenolic oxygen-rich compounds, i.e., compounds likely enriched in aromatic structures (Fig. 4*A*, $P < 0.001$), as expected if there was a greater contribution of surficial soil layers and harvest residues to the DOM pool. We also found evidence for contributions from deeper soil layers. On average, N-containing DOM from the logged catchments in this study comprised 43% of the newly added compounds, but only 32% of all identified compounds (Fig. 4*B* and *SI Appendix*, Tables S8 and S9). Most of the added N-compounds fell outside of the H:C range interpreted as being associated with autochthonous inputs from primary production (55) (Fig. 4*A*). Instead, higher N content likely corresponded with release of aged organic carbon (7) through disturbance of deeper soils. The concomitant increase in carboxyl-rich alicyclic molecules (CRAMs) supports this hypothesis, as the relative intensity of CRAMs increases with microbial processing of carbon and is known to be greater in deeper soils (43, 56).

To test further whether the increased chemodiversity originated from soils after logging, we tracked DOM from soils into streams monthly during the experiment. We did so by installing lysimeters at four depths at four hillslope positions in all four catchments (see ref. 43). At each time point, we compared the similarity between all soil samples (n = 16) and the stream within a catchment (16 pairs × 4 catchments), integrating these two sample types only for this analysis. We found that the similarity in the molecular composition of DOM between catchment soils and streams persisted in harvest sites compared to controls after logging, suggesting higher hydrological connectivity (Fig. 5*A* and *SI Appendix*, Table S10, $P < 0.001$). The connectivity between streams and soils in the harvested sites likely arose from intermediate (15 cm) and deep (60 cm) soils remaining connected to streams, given the similarity in DOM composition at these depths in the harvest sites compared to the controls postlogging (Fig. 5*B*, $P = 0.005$-0.009). By contrast, streams in unharvested sites declined in their similarity to catchment soils over this same time period from a mean of 60% (95% CI: 58 to 63%) similarity before logging to 53% (95% CI: 51 to 56%) afterward (Fig. 5*A* and *SI Appendix*, Table S11, $P = 0.263$). This loss in similarity is consistent with the decline in compound count being attributed to fewer hydrologically connected source areas in the control versus harvest catchments as expected later in the season [(57, 58) and *SI Appendix*, Fig. S4]. These results build on the surface contribution model (59), often used to explain increased DOM concentrations after harvest (3, 60)

An alternative explanation for the higher compound count and maintained soil-stream similarity in the harvest sites relative to the controls is that tire or track forces from harvest machinery caused soil displacement and rut formation (61–64). Rutting may partly be responsible for the signal from deeper soils, as ruts on slopes are preferential routes for runoff, which become deeper because of erosion (65). By contrast, woody debris left by harvest operations at the soil surface may have contributed to the increased representation of polyphenols (66, 67). However, only between 15% and 18% of foliage and fine roots leftover by harvest may be lost annually (68) and so these sources may have contributed little to DOM changes in our experiment.

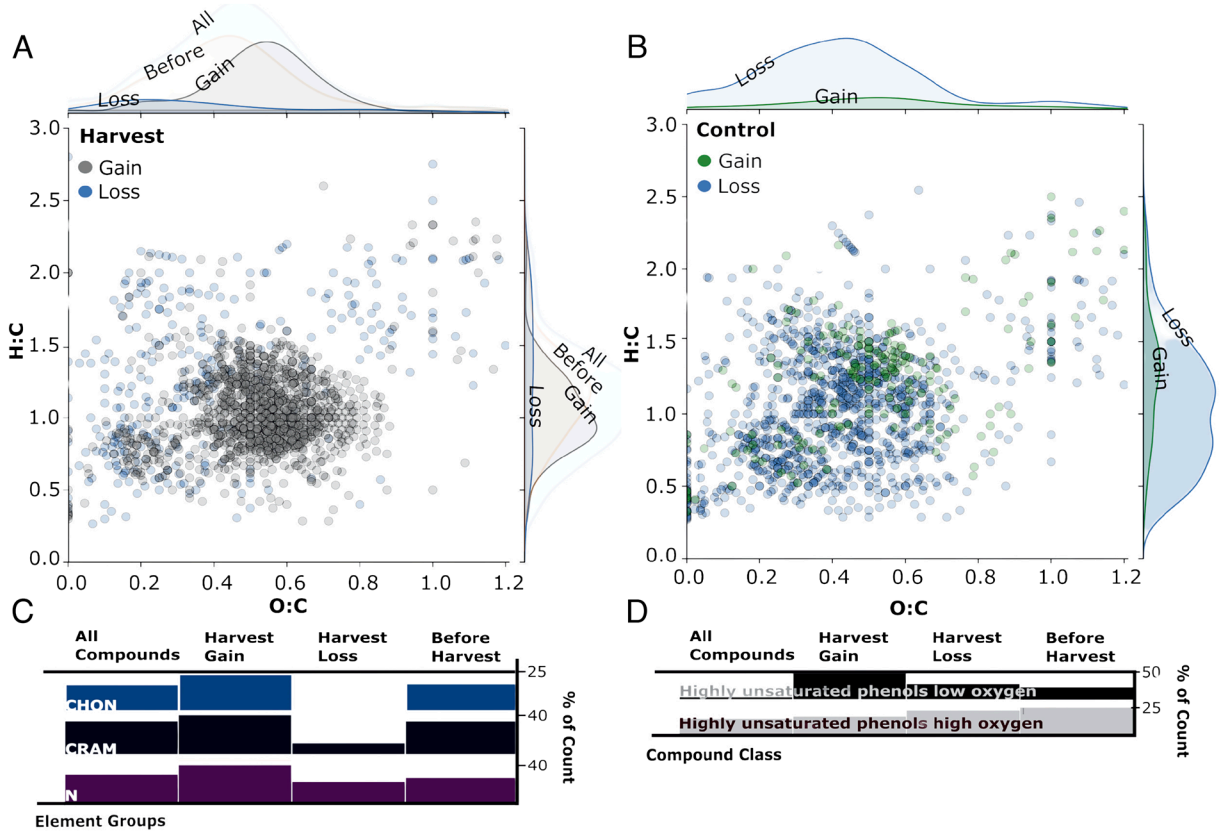

Fig. 4. Harvest increases the chemodiversity of stream DOM by introducing compounds reflective of fresh plant material and disturbed soil. Elemental ratios of molecular formulae detected in (*A*) harvest and (*B*) control sites. Probability densities are given along each axis for compounds gained after harvest only in harvest sites (gray, n = 1,035) and gained after the harvest period only in control sites (green, n = 220), for compounds lost only in harvest (blue, n = 320) and control (blue, n = 962) sites, and all compounds present in the harvest site before logging [n = 4,927, (*A*) only]. We also plotted the percentage of all compounds (n = 7,444) that contained (*C*) different elements (*SI Appendix*, Table S8) or classified into (*D*) different compound classes (*SI Appendix*, Table S9). Ticks are aligned to the highest bar in each row. The base of the bars equals 0%.

Discussion

By disrupting soil, our study indicates forest harvest breaches spatial barriers that would otherwise isolate SOM from aquatic ecosystems. In deeper soil horizons, SOM is typically stabilized via organo-mineral complexation alongside physical disconnection from decomposers and enzymes (69). Logging activity removes surface soils, exposing deeper layers (as with ruts) to disrupt physical protection of SOM by destabilizing aggregate structures. Logging can also bring deeper layers to the surface, resulting in the chemical disruption of organo-mineral complexes through changes in redox potential, pH, and oxygen availability. Together, the loss of

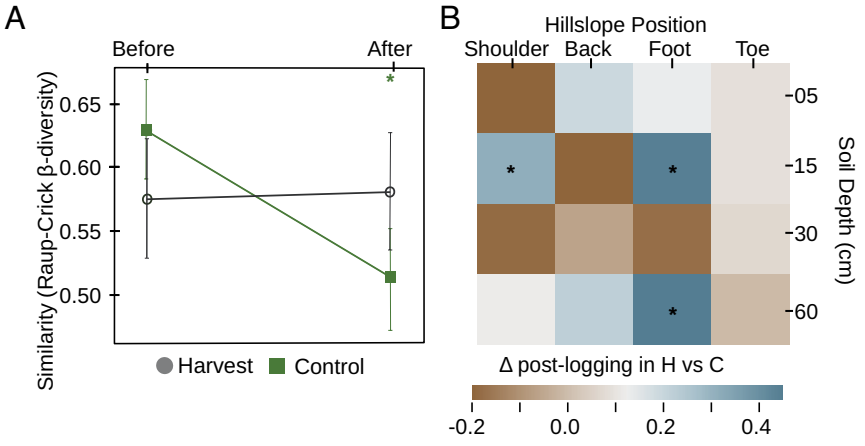

Fig. 5. Harvest maintains similarity in DOM composition between stream and soil waters. We calculated the similarity between the molecular composition of DOM in streams and porewater at each soil position (n = 4 depths × 4 hillslopes) in each catchment (n = 4), accounting for differences solely because of differing numbers of compounds in a sample. (*A*) We estimated mean (±95% CI) similarity across all time points both before (n = 5) and after (n = 3) logging in 2020. * indicates a statistically significant difference ($P < 0.05$) between before and after forest harvest (*SI Appendix*, Table S11). (*B*) Changes in molecular composition of DOM after logging in harvest versus the control sites for each depth-by-hillslope combination averaged across catchments. Positive values indicate greater differences in DOM composition after logging in harvest (H) than in control (C) treatments, whereas negative values indicate the reverse. *statistically significant difference in soil-stream similarity between the before and after period between treatments ($P < 0.05$, *SI Appendix*, Table S11).

protections to deep soil DOM may result in its export to aquatic ecosystems where it becomes more bioavailable (59). Here, we also found that DOM from harvested catchments had unique molecular formulae relative to unharvested catchments and these formulae were absent in the streams prior to harvest. This pulse of unique molecules to streams could have unexpected consequences on their ecology of molecules, analogous to species introductions in biological communities (70). The unique compounds from typically unconnected soil environments may impact stream microbial communities differently than in the compounds' native soil "ranges," potentially reshuffling the network of relationships among DOM compounds and stream microorganisms (17, 71). Uncovering the relationship between molecules uniquely derived from deep soils and stream microbial communities is a necessary next step in quantifying aquatic carbon losses following disturbances such as forest harvest.

Our results directly address key knowledge gaps that have been identified for accurate national and international carbon accounting. Integration of inland freshwater ecosystems, in general, has been identified as a critical knowledge gap in carbon accounting models (72), with the fate of forest-derived carbon in water recognized as critical to resolve, see ref. 73 goal 9. There is a long history of managing forests for the protection of water resources in many countries through BMPs primarily targeting the reduction of soil disturbance, the retention of riparian buffer strips, and the reduction of road-related runoff (74). While these BMPs are generally effective at reducing sedimentation (75, 76), we show that those using low-impact selection cut techniques in hardwood stands still result in a large release of carbon to water in forms that are more susceptible to microbial transformation. A key uncertainty to resolve will be whether the eventual fate of this carbon differs from that in forest soils. This outcome will depend on the balance between particulate versus mineral-associated organic matter. Mineral-associated organic matter dominates our study sites (approximately 60% of total organic matter; refs. 77 and 78), along with temperate and continental climates globally (79). Thus, our findings improve our understanding of the fate of aquatic carbon in forest carbon accounting and highlight the need to consider these linkages if forest management is to be an effective natural climate solution.

The effects we observed in our studied stream reaches are applicable to the effective implementation of natural climate solutions within these and similar (hemi)boreal forest ecosystems. Furthermore, our results highlight processes that should be considered when evaluating natural climate solutions in other biomes given regional variation in the response of DOM to logging (6, 7). By intersecting maps of global harvest area (80) with the distribution of headwater streams (81), we estimated that ca. 10% of managed forests are drained by similar waterways to those that we studied. Although rotation time can be as much as 100 y or more in these forests (82), around 15.5 (80) and 0.7 (83) Mha of global and Canadian land area is harvested annually in similar or greater proportions to that observed here, respectively. This frequency creates a continuous mosaic of landscape patches in different stages of recovery, which can take 10 to 20 y to revert to a carbon sink (84). Our results demonstrate that without consideration and inclusion of aquatic carbon fluxes as part of BMPs, the potential carbon sequestration from wood harvest, particularly in northern regions like those examined here, will be miscalculated.

Materials and Methods

Overview of Study Design. We used a BACI experiment to test how logging impacts DOM in forest headwater streams. The design compares DOM collected before and after a logging impact with measurements from unlogged control areas. Consequently, it can account for natural background changes that occur over time between the period before versus after the impact. We selected two impact catchments, each with a single headwater stream, and paired each with a nearby control catchment based on similar characteristics, including topography, forest composition, and soil type (*SI Appendix, Supplementary Methods*). The paired approach minimizes confounding factors and ensures differences between catchments are primarily related to the experimental impact. We collected water from the channel head of each headwater stream and from soils at four hillslope positions and four depths per position (see *SI Appendix*, Fig. S6 for spatial representation of sampling locations). Samples were collected in September and October 2019 (total n = 2 samples per stream), June to November (and twice in October) in 2020 (n = 7), and monthly during the ice-free season in the year after logging (2021, total n = 6). We measured water chemistry, including DOM concentration, and both the optical properties and molecular composition of DOM of all samples.

Site Description and Selection. The four experimental hardwood-dominated catchments were located northeast of Lake Superior, ON, Canada (Fig. 1) on the hemiboreal transition between the Great Lakes-St. Lawrence Forest Region and the Boreal Forest Region; the two largest forest regions in Canada (85). Catchments ranged in size from 0.115 to 0.140 km^2, with a mean area of 0.128 km^2 (*SI Appendix*, Table S12), and were within the larger Batchawana Watershed due to the presence of the Turkey Lakes Watershed (TLW, 10.5 km^2) experimental study (86). TLW was established in 1979 and is one of the longest running watershed-based ecosystem studies in Canada (87). The extensive scientific and support infrastructure at TLW hosts a comprehensive environmental data record which we utilized to estimate C fluxes and understand likely baseline conditions for our sites. The forests of the regions consist of uneven-aged hardwood forests with primarily podzolic (spodosols) soils with well-developed forest floor horizons (88). We focus this study on hardwood-dominated forests in this hemiboreal region because of the expected shift toward hardwood species in temperate forests and the associated increased pressure on hardwood forests (89), and because this forest region is expected to undergo particularly rapid climate shifts (90). The most recent operational logging occurred in the 1950s when the area was selectively logged for high-quality yellow birch (*Betula alleghaniensis*), sugar maple (*Acer saccharum*), white spruce (*Picea glauca*), and white pine (*Pinus strobus*) (91).

To select experimental catchments, the regional commercial forestry company (Boniferro Mill Works Inc., Sault Ste. Marie, ON) provided historical and future harvest plans. Within the future harvest region, we delineated catchments of headwater streams. Catchment boundaries were delineated using WhiteboxTools (92), a python scripting API for geospatial analysis, along with 30 m digital elevation models (DEMs) from the Government of Ontario and existing hydrological data from the Ontario Integrated Hydrology (OIH) dataset. Flow accumulation and flow pointer grids were generated using the D8 algorithm, where flow entering each cell is routed to only a single downstream neighbor (93). Streams were extracted using the generated flow accumulation map and a threshold value of 0.128 km^2. This threshold value was selected by stepping through values and visually validating the generated network against satellite images of streams, catchments generated in smaller areas from 5 m LiDAR-derived DEMs available for the TLW, and the stream network shape from the OIH dataset.

We then matched the harvest catchments to control catchments by maximizing their similarity in a) topography, b) forest composition, and c) ecosite composition. Topography results were generated for each grid cell in the input DEM and included the slope gradient (i.e., steepness in degrees), aspect, sediment transport index, topographic wetness index, and Pennock landform classification (94). For each topographic variable we calculated median, maximum, minimum, and SD values which were then assigned to the derived catchments. Forest composition was measured from the Ontario Forest Resources Inventory (FRI). This inventory is based on digital aerial photo interpretation and field surveys, with a recent incorporation of LiDAR data. From this layer we extracted polygons of overstory and understory species composition (and averaged the percent composition when both were available for a single site), tree species identified in the stand (or the uppermost canopy if the stand contained two or more distinct layers), and the percent cover each tree species occupies within the canopy. Additionally, we utilized the primary ecosite attribute from the FRI database. Ecosite is defined as an ecological unit composed of relatively uniform geology, parent material, soils, topography, and hydrology and consists of related vegetation conditions. An intersection function was then used to calculate the percentage of area contributed by each tree species and ecosite to the catchment. We excluded possible

control catchments based on a 300 m distance to a passable road (a semiarbitrary threshold selected based on logistical concerns). Road data were downloaded from the Ministry of Natural Resources. Catchments within 50 m of the DEM edge were also removed to avoid edge effects. These steps left n = 2,177 catchments for further selection.

Control catchments were then selected using a divisive (top–down) hierarchical clustering analysis. This procedure is defined by a stepwise algorithm which starts with one cluster of all observations, and splits clusters into subgroups with each successive step based on within-group similarity and intergroup distance defined by the Ward's method linkage and Euclidean distance, respectively. Permutations continued until there was only a single catchment remaining in the same branch/cluster as the catchments selected for harvest.

Within each of the four experimental catchments, hillslopes were further partitioned into four topographic features for soil water collection based on morphological features of surface DEMs according to Conacher and Dalrymple 1977 (95) and the Height Above the Nearest Drainage (HAND) terrain model (96). The HAND model correlates with the depth of the water table, providing a spatial representation of soil water environments (k = 42 clusters) (97). The four features were shoulder, backslope, footslope, and toeslope.

Logging. Harvest operations were performed across the entirety of each catchment according to the Ontario Stands and Site Guide for tolerant hardwood selection cuts (98). Selection cut aims to remove, on average, 30% of the total basal area of tree stems in a stand but never more than 33%. Trees were felled by an Avery Tigercat LX380D feller buncher. Limbs were removed on site, and the tree-length stems were forwarded to roadside landings by rubber-tired skidders with tire chains. Operators were careful to avoid driving machinery into or across stream beds with adherence to the Ontario Stands and Site Guide (98), including leaving 30 m buffers on all mapped or obvious watercourses and avoidance of sensitive wet soils.

Stream Water Samples. Stream water samples were collected monthly during ice-free seasons beginning in September 2019. Surface water (500 mL) was grab-sampled from a single location at the channel head of each stream. DOM quantification and molecular characterization was performed on water filtered through 0.45 μm glass fiber syringe filters (Kinesis Inc., USA) into precombusted (4 h, 400 °C) amber vials. Samples for molecular characterization were acidified to pH 2 with HCl within 24 h. Samples were stored at 4 °C in the dark until analysis within 4 mo with no flocculation observed. DOM was quantified using a Shimadzu TOC-L (Shimadzu, Japan) with concentrations determined via an L-arginine standard curve. For molecular characterization in 2020 only, we extracted 10 mL of each sample onto 100 mg solid-phase extraction columns (Bond Elut PPL, Agilent) and eluted the samples with 3 mL methanol (ULC grade) using the methods described by Dittmar et al. (99). We also characterized DOM with optical analyses of filtered and refrigerated nonacidified water described above across all three study years. Three-dimensional fluorescence scans were performed using a Cary Eclipse (Varian Instruments, USA), and absorbance measured with a Cary 60 UV–Vis (Agilent Technologies, USA). Fluorescence scans were run at 5 nm excitation steps from 250 to 450 nm, and emissions were read at 2 nm steps from 300 to 600 nm. Spectral corrections (instrument and inner-filter), and calculation of the HIX (40) were applied following standard procedures using the staRdom R package (100). Finally, major ions, nutrients, and metal concentrations were measured from a subset of the sampled water collected in all years at the Great Lakes Forestry Centre, Sault Ste. Marie, ON, according to methods outlined in ref. 43.

Soil Water Collection. At all hillslope positions, at least 60 mL of soil water was sampled at 15, 30, and 60 cm depths with tension lysimeters. The lysimeters consisted of 60-mm-long round-bottom-necked porous cups with an outer diameter of 48 mm and an effective pore size of 1.3 μm (model 0653X01-B02M2, Soilmoisture Equipment Corp.). Lysimeters were installed 6 to 12 wk prior to first sampling using a slurry of nontreated native soil. All lysimeters were evacuated at least twice prior to first sampling to allow for calibration (101). The sampling bottles were evacuated to a negative pressure of 50 kPa with a hand pump, so suction pressure was ca. 50 mbar above the actual soil water tension at collection. At 5 cm depths, lysimeters could not be securely installed. Therefore, we sampled pore water with microtensiometers designed to extract fluids nondestructively from soils using a vacuum (102) through a 0.6 μm ceramic cup (Rhizon CSS samplers, Rhizosphere Research Products, Netherlands). All the water samplers were installed in triplicate and water pooled at each of the four depth and position combinations to retrieve sufficient volume for analysis. The hillside design of 16 soil samples and 1 stream sample was replicated across the 4 catchments for a total number of 68 samples per sampling date. Soil water samples were filtered through a 0.45 μm glass fiber filter, acidified (pH 2), and stored at 4 °C prior to subsequent analyses of DOM concentration and molecular characterization. Sample water for DOM optical analyses were refrigerated but not acidified. DOM optical analysis, major ions, nutrients, and metals were analyzed methods described in the previous section.

FT-ICR MS Analysis. We analyzed individual stream samples (n = 4 catchments × 7 dates) and soil extracts pooled across replicate lysimeters at each hillslope and depth (n = 68 samples × 7 dates), all collected in 2020, using FT-ICR MS. The analysis was performed on a 15 T Solarix (Bruker Daltonics, USA) equipped with an electrospray ionization source (ESI, Bruker Apollo II) applied in negative ionization mode. Samples were diluted to yield a concentration of ~5 ppm in ultrapure water and methanol 50:50 (vol/vol). This dilution was filtered through precleaned and rinsed 0.2 μm polycarbonate syringe filters before samples were analyzed in duplicate and in random order Electrospray ionization in negative mode (Bruker Apollo II) was done at 200 °C and the capillary voltage was set to 4.5 kV. The sample was injected at a flow rate of 120 $\mu L\ h^{-1}$, the accumulation time was set to 0.05 s, and 200 scans were coadded for each spectrum in a mass range of 92 to 2,000 Da. Mass spectra were exported from the Bruker Data Analysis software at a signal-to-noise ratio of 0 and molecular formulae were assigned using the ICBM-OCEAN tool (103). The method detection limit was set to 3. Junction of mass lists along mass to charge ratios (m/z) was performed via fast join at a tolerance of 0.5 ppm while standard smooth and additional isotope tolerance was 10‰. Singlet peaks occurring only once in the dataset were removed, then molecular formulae were assigned with a tolerance of 0.5 ppm in the range m/z 0 to 1,000 within the limits $C_{1-100}H_{1-100}O_{0-70}N_{0-4}S_{0-2}P_{0-1}$. Before statistical analysis, relative intensities were normalized to the sum of intensities per sample. Furthermore, molecular formulae were only retained in the dataset if they occurred at least three times across all stream or porewater samples.

For each molecular formula, we calculated 10 traits related to molecular weight, stoichiometry, chemical structure, and oxidation state. These traits were molecular mass, the heteroatom class, double bond equivalents [DBE = number of rings plus double bonds to carbon, double bond equivalent (DBE) (104)], carbon number (C), GFE of carbon oxidation (105), nominal oxidation state of carbon (NOSC), O:C ratio, H:C ratio, and AI_{mod} (42, 106). Molecules were classified as CRAM where DBE:C was between 0.30 and 0.68, DBE:H was between 0.20 and 0.95 and DBE:O were between 0.77 and 1.75 (107). Formulae with $AI_{mod} \leq 0.5$, $0.5 <$ to ≤ 0.66, and >0.66 were defined as highly unsaturated and phenolics, polyphenolic, and condensed aromatic, respectively. Formulae with $1.5 \leq$ H:C ≤ 2.0, O:C ≤ 0.9, and N = 0 were defined as aliphatic (108).

To compare DOM between each soil sample and stream at each time point, we calculated the Raup–Crick dissimilarity metric β_{RC} (109). This metric estimates whether pairwise samples are more different in composition than expected by chance, given random draws from the compound pool at a site. For any given pair of soil and stream samples, β_{RC} was calculated by comparing the observed number of shared molecular formulae to the number expected by randomly sampling the same number in each site from the entire compound pool following the protocol described in ref. 109. The probability of sampling a compound was based on its abundance across all soil sites. We repeated this sampling 1,000 times to measure the similarity between the molecular composition of DOM in streams and soils compared to a null expectation. To avoid overestimating differences between samples, we used presence–absence of formulae rather than their relative abundance as recommended by ref. 110.

DOM Yield and Wood Carbon Estimates. DOM yields for each of the four experimental catchments were estimated using runoff data from the nearby TLW (58) where monthly runoff and precipitation values ($mm\ mo^{-1}$) are measured (*SI Appendix*, Fig. S4). Catchments in the TLW have similar size (ranging from 0.04 to 0.40 km^2, median = 0.02 km^2, mean = 0.06 km^2 and forest composition as our study catchments). Runoff from TLW catchments was measured using stage-discharge relationships at 90° V-notch weirs, with stage measured at 10 min intervals using water level recorders described in refs. 58 and 111. We normalized

estimated runoff volume by the annual precipitation measured across 3 y (mm, 2019–2021). Carbon concentration increases were converted to volume using a 1,000 L m^{-3} conversion. To estimate extra carbon exported from each experimental catchment (mg C mo^{-1} km^{-2}), we multiplied the observed carbon increase (assuming 50% carbon content in DOM, or approximately 1.2 mg L^{-1} C increase; Fig. 1*B* and *SI Appendix*, Table S1) over 8 nonwinter months by the estimated monthly runoff volume (L mo^{-1} km^{-2}).

We estimated the amount of tree carbon removed from the two logged experimental catchments using an estimate of aboveground phytomass for the region described within ref. 112. Phytomass was then converted to carbon using a 50% (w/w) dry wood conversion based on the canopy-dominant sugar maple (113).

Statistical Analyses. To test the effects of logging on stream water chemistry and DOM (including concentration, optical properties, compound counts, and molecular dissimilarity), we fitted linear mixed effects models. The time period (before or after logging) and treatment (control or impact, i.e., logging) were fixed effects, and we included the interaction between these two variables. We also included the number of days since logging as a continuous predictor, whereby the slope of this effect represented the rate of change in DOM concentration over time. Finally, we included the three-way interaction among the number of days since logging and the two factors, i.e., before-after × control-impact × time, as described in ref. 114. This model design allowed us to estimate the specific times when differences arose between treatments, such as from before-after × time or control-impact × time interactions. We accounted for repeat sampling of the same sites through time by including a site-level random effect and estimated a continuous autoregressive correlation structure to account for temporal autocorrelation within year and site. Finally, for water chemistry and optical properties that were measured throughout the entire study period, we fitted a separate model to 2020 data only and from 2019 to 2021 to separate short- versus long-term effects of logging. These models had the additional advantage of analyzing the exact same period for which we collected FT-ICR MS data (2020 only) while also extending across the entire study period.

Models were fitted with the lme function in the nlme (115) package in R (116). Only when the predicted variable was a count (i.e., number of molecular formulae), we modeled the error terms using a Poisson distribution and estimated statistical models using the R package glmmTMB (117). The nlme package does not support Poisson error structures. Concurrently, we did not use glmmTMB for all other statistical models (e.g., DOM concentration, optical indices) since it does not allow for a continuous correlation structure with time, which is important for capturing the structure of our data. In the case of the Poisson-distributed models fitted with glmmTMB, we instead used ordinal values (order of sample points in time) to model the autoregressive temporal correlation structure as properly modelling the error distribution was considered to be more important.

Data, Materials, and Software Availability. Raw and Processed data have been deposited in 10.5281/zenodo.16677581 (118).

ACKNOWLEDGMENTS. We are thankful to K. Klapproth and I Ulber for assistance with FT-ICR-MS measurements and to Irena F. Creed for sending much-needed field support. We thank Mike Thompson and Jason McLellan for contributing the harvest in the "harvest experiment." We also thank the staff at the Natural Resources Canada–Canadian Forest Service for considerable support, including with logistics and advice (Paul Hazlett, Dan McKenney, John Pedlar, Jason Leach, and Rob Fleming) and general field and laboratory assistance (J. Schadenberg, D. Chartrand, Caroline Emilson, Ken McIlwrick, and many others).

Author affiliations: [a]Ecosystems and Global Change Group, Department of Plant Sciences, University of Cambridge, Cambridge CB2 3EA, United Kingdom; [b]Department of Aquatic Ecology, Eawag, Swiss Federal Institute of Aquatic Science and Technology, Dübendorf CH-8600, Switzerland; [c]Natural Resources Canada, Canadian Forest Service, Great Lakes Forestry Centre, Sault Ste. Marie, ON P6A 2E5, Canada; [d]Ecosystems and Global Change Group, School of the Environment, Trent University, Peterborough, ON K9L 0G2, Canada; [e]Institute for Chemistry and Biology of the Marine Environment, University of Oldenburg, Oldenburg 26129, Germany; and [f]Helmholtz Institute for Functional Marine Biodiversity at the University of Oldenburg, Oldenburg 26129, Germany

1. P. Nepal, C. M. T. Johnston, I. Ganguly, Effects on global forests and wood product markets of increased demand for mass timber. *Sustain. Sci. Pract. Policy* **13**, 13943 (2021).
2. A. Mishra *et al.*, Land use change and carbon emissions of a transformation to timber cities. *Nat. Commun.* **13**, 4889 (2022).
3. J. Schelker, K. Eklöf, K. Bishop, H. Laudon, Effects of forestry operations on dissolved organic carbon concentrations and export in boreal first-order streams. *J. Geophys. Res.* **117**, 2011JG001827 (2012).
4. D. P. Kreutzweiser, P. W. Hazlett, J. M. Gunn, Logging impacts on the biogeochemistry of boreal forest soils and nutrient export to aquatic systems: A review. *Environ. Rev.* **16**, 157–179 (2008).
5. A. Deininger, A. Jonsson, J. Karlsson, A.-K. Bergström, Pelagic food webs of humic lakes show low short-term response to forest harvesting. *Ecol. Appl.* **29**, e01813 (2019).
6. J. L. Meyer, C. M. Tate, The effects of watershed disturbance on dissolved organic carbon dynamics of a stream. *Ecology* **64**, 33–44 (1983).
7. T. W. Drake *et al.*, Mobilization of aged and biolabile soil carbon by tropical deforestation. *Nat. Geosci.* **12**, 541–546 (2019).
8. M. Nakhavali *et al.*, Leaching of dissolved organic carbon from mineral soils plays a significant role in the terrestrial carbon balance. *Glob. Chang. Biol.* **27**, 1083–1096 (2020).
9. D. Caissie, S. Jolicoeur, M. Bouchard, E. Poncet, Comparison of streamflow between pre and post timber harvesting in Catamaran Brook (Canada). *J. Hydrol.* **258**, 232–248 (2002).
10. M. J. Waterloo, J. Schellekens, L. A. Bruijnzeel, T. T. Rawaqa, Changes in catchment runoff after harvesting and burning of a Pinus caribaea plantation in Viti Levu, Fiji. *For. Ecol. Manage.* **251**, 31–44 (2007).
11. J. M. Buttle, "The effects of forest harvesting on forest hydrology and biogeochemistry" in *Forest Hydrology and Biogeochemistry: Synthesis of Past Research and Future Directions*, D. F. Levia, D. Carlyle-Moses, T. Tanaka, Eds. (Springer Netherlands, 2011), pp. 659–677.
12. T. J. Battin *et al.*, River ecosystem metabolism and carbon biogeochemistry in a changing world. *Nature* **613**, 449–459 (2023).
13. S. Tao, Water soluble organic carbon and its measurement in soil and sediment. *Water Res.* **34**, 1751–1755 (2000).
14. T. Dittmar *et al.*, Enigmatic persistence of dissolved organic matter in the ocean. *Nat. Rev. Earth Environ.* **2**, 570–583 (2021).
15. E. C. Freeman, T. Peller, F. Altermatt, Ecosystem ecology needs an ecology of molecules. *Trends Ecol. Evol.* **40**, 219–223 (2025).
16. A. Hu *et al.*, Microbial and environmental processes shape the link between organic matter functional traits and composition. *Environ. Sci. Technol.* **56**, 10504–10516 (2022).
17. A. Hu, F. Meng, A. J. Tanentzap, K.-S. Jang, J. Wang, Dark matter enhances interactions within both microbes and dissolved organic matter under global change. *Environ. Sci. Technol.* **57**, 761–769 (2023).
18. A. J. Tanentzap *et al.*, Chemical and microbial diversity covary in fresh water to influence ecosystem functioning. *Proc. Natl. Acad. Sci. U.S.A.* **116**, 24689–24695 (2019).
19. R. Flerus *et al.*, A molecular perspective on the ageing of marine dissolved organic matter. *Biogeosciences* **9**, 1935–1955 (2012).
20. O. J. Lechtenfeld *et al.*, Molecular transformation and degradation of refractory dissolved organic matter in the Atlantic and Southern Ocean. *Geochim. Cosmochim. Acta* **126**, 321–337 (2014).
21. S. Kim, L. A. Kaplan, P. G. Hatcher, Biodegradable dissolved organic matter in a temperate and a tropical stream determined from ultra-high resolution mass spectrometry. *Limnol. Oceanogr.* **51**, 1054–1063 (2006).
22. J. D'Andrilli, W. T. Cooper, C. M. Foreman, A. G. Marshall, An ultrahigh-resolution mass spectrometry index to estimate natural organic matter lability. *Rapid Commun. Mass Spectrom.* **29**, 2385–2401 (2015).
23. S. R. Textor, K. P. Wickland, D. C. Podgorski, S. E. Johnston, R. G. M. Spencer, Dissolved organic carbon turnover in permafrost-influenced watersheds of interior Alaska: Molecular insights and the priming effect. *Front. Earth Sci.* **7**, 275 (2019).
24. A. Mostovaya, B. Koehler, F. Guillemette, A.-K. Brunberg, L. J. Tranvik, Effects of compositional changes on reactivity continuum and decomposition kinetics of lake dissolved organic matter. *J. Geophys. Res. Biogeosci.* **121**, 1733–1746 (2016).
25. A. Mostovaya, J. A. Hawkes, B. Koehler, T. Dittmar, L. J. Tranvik, Emergence of the reactivity continuum of organic matter from kinetics of a multitude of individual molecular constituents. *Environ. Sci. Technol.* **51**, 11571–11579 (2017).
26. J. A. Downing *et al.*, Global abundance and size distribution of streams and rivers. *Inland Waters* **2**, 229–236 (2012).
27. C. Blattert *et al.*, Climate targets in European timber-producing countries conflict with goals on forest ecosystem services and biodiversity. *Commun. Earth Environ.* **4**, 1–12 (2023).
28. A. Stubbins *et al.*, What's in an EEM? Molecular signatures associated with dissolved organic fluorescence in boreal Canada. *Environ. Sci. Technol.* **48**, 10598–10606 (2014).
29. A. J. Underwood, On beyond BACI: Sampling designs that might reliably detect environmental disturbances. *Ecol. Appl.* **4**, 3–15 (1994).
30. S. D. Sebestyen *et al.*, Sources, transformations, and hydrological processes that control stream nitrate and dissolved organic matter concentrations during snowmelt in an upland forest. *Water Resour. Res.* **44**, 2008WR006983 (2008).
31. J. Seibert *et al.*, Linking soil- and stream-water chemistry based on a riparian flow-concentration integration model. *Hydrol. Earth Syst. Sci.* **13**, 2287–2297 (2009).
32. C. M. T. Johnston, V. C. Radeloff, Global mitigation potential of carbon stored in harvested wood products. *Proc. Natl. Acad. Sci. U.S.A.* **116**, 14526–14531 (2019).
33. Q. Zhang *et al.*, Global timber harvest footprints of nations and virtual timber trade flows. *J. Clean. Prod.* **250**, 119503 (2020).
34. J. Zhao, X. Wei, L. Li, The potential for storing carbon by harvested wood products. *Front. For. Glob. Change* **5**, 1055410 (2022).
35. P. Brunet-Navarro, H. Jochheim, G. Cardellini, K. Richter, B. Muys, Climate mitigation by energy and material substitution of wood products has an expiry date. *J. Clean. Prod.* **303**, 127026 (2021).
36. L. Gustavsson, K. Pingoud, R. Sathre, Carbon dioxide balance of wood substitution: Comparing concrete- and wood-framed buildings. *Mitig. Adapt. Strateg. Glob. Chang.* **11**, 667–691 (2006).
37. M. B. Mills *et al.*, Tropical forests post-logging are a persistent net carbon source to the atmosphere. *Proc. Natl. Acad. Sci. U.S.A.* **120**, e2214462120 (2023).
38. J. James, R. Harrison, The effect of harvest on forest soil carbon: A meta-analysis. *Forests* **7**, 308 (2016).

39. G. Aiken, "fluorescence and dissolved organic matter" in *Aquatic Organic Matter Fluorescence*, P. G. Coble, J. Lead, A. Baker, D. M. Reynolds, R. G. M. Spencer, Eds. (*Cambridge Environmental Chemistry Series*, Cambridge University Press, 2014), pp. 35–74.
40. T. Ohno, Fluorescence inner-filtering correction for determining the humification index of dissolved organic matter. *Environ. Sci. Technol.* **36**, 742–746 (2002).
41. C. Patriarca *et al.*, Investigating the ionization of dissolved organic matter by electrospray. *Anal. Chem.* **92**, 14210–14218 (2020).
42. B. P. Koch, T. Dittmar, From mass to structure: An aromaticity index for high-resolution mass data of natural organic matter. *Rapid Commun. Mass Spectrom.* **20**, 926–932 (2006).
43. E. C. Freeman *et al.*, Universal microbial reworking of dissolved organic matter along environmental gradients. *Nat. Commun.* **15**, 187 (2024).
44. L. P. P. Braga *et al.*, Viruses direct carbon cycling in lake sediments under global change. *Proc. Natl. Acad. Sci. U.S.A.* **119**, e2202261119 (2022).
45. E. M. Thurman, "Amount of organic carbon in natural waters" in *Organic Geochemistry of Natural Waters*, E. M. Thurman, Ed. (Springer Netherlands, 1985), pp. 7–65.
46. R. Benner, "Molecular indicators of the bioavailability of dissolved organic matter" in *Aquatic Ecosystems*, S. E. G. Findlay, R. L. Sinsabaugh, Eds. (*Aquatic Ecology*, Academic Press, 2003), pp. 121–137.
47. H.-S. Song *et al.*, Representing organic matter thermodynamics in biogeochemical reactions via substrate-explicit modeling. *Front. Microbiol.* **11**, 531756 (2020).
48. E. B. Graham *et al.*, Potential bioavailability of representative pyrogenic organic matter compounds in comparison to natural dissolved organic matter pools. *Biogeosciences* **20**, 3449–3457 (2023).
49. R. E. Danczak *et al.*, Using metacommunity ecology to understand environmental metabolomes. *Nat. Commun.* **11**, 6369 (2020).
50. J. D. Fudyma, R. K. Chu, N. Graf Grachet, J. C. Stegen, M. M. Tfaily, Coupled biotic–abiotic processes control biogeochemical cycling of dissolved organic matter in the Columbia River hyporheic zone. *Front. Water* **2**, 574692 (2021).
51. R. Breitling, S. Ritchie, D. Goodenowe, M. L. Stewart, M. P. Barrett, Ab initio prediction of metabolic networks using Fourier transform mass spectrometry data. *Metabolomics* **2**, 155–164 (2006).
52. L. M. Lynch *et al.*, River channel connectivity shifts metabolite composition and dissolved organic matter chemistry. *Nat. Commun.* **10**, 459 (2019).
53. A. M. Kellerman *et al.*, Unifying concepts linking dissolved organic matter composition to persistence in aquatic ecosystems. *Environ. Sci. Technol.* **52**, 2538–2548 (2018).
54. A. Stubbins *et al.*, Illuminated darkness: Molecular signatures of Congo River dissolved organic matter and its photochemical alteration as revealed by ultrahigh precision mass spectrometry. *Limnol. Oceanogr.* **55**, 1467–1477 (2010).
55. A. Mostovaya, J. A. Hawkes, T. Dittmar, L. J. Tranvik, Molecular determinants of dissolved organic matter reactivity in lake water. *Front. Earth Sci.* **5**, 106 (2017).
56. X. Zhang *et al.*, Importance of lateral flux and its percolation depth on organic carbon export in Arctic tundra soil: Implications from a soil leaching experiment. *J. Geophys. Res. Biogeosci.* **122**, 796–810 (2017).
57. I. F. Creed, T. Hwang, B. Lutz, D. Way, Climate warming causes intensification of the hydrological cycle, resulting in changes to the vernal and autumnal windows in a northern temperate forest: Climate warming causes hydrological intensification in forests. *Hydrol. Process.* **29**, 3519–3534 (2015).
58. J. A. Leach, D. T. Hudson, R. D. Moore, Assessing stream temperature response and recovery for different harvesting systems in northern hardwood forests using 40 years of spot measurements. *Hydrol. Process.* **36**, e14753 (2022).
59. C. Rumpel, I. Kögel-Knabner, Deep soil organic matter–A key but poorly understood component of terrestrial C cycle. *Plant Soil* **338**, 143–158 (2011).
60. M. A. Burns, H. R. Barnard, R. S. Gabor, D. M. McKnight, P. D. Brooks, Dissolved organic matter transport reflects hillslope to stream connectivity during snowmelt in a montane catchment. *Water Resour. Res.* **52**, 4905–4923 (2016).
61. R. Horn, J. Vossbrink, S. Peth, S. Becker, Impact of modern forest vehicles on soil physical properties. *For. Ecol. Manage.* **248**, 56–63 (2007).
62. J. Vossbrink, R. Horn, Modern forestry vehicles and their impact on soil physical properties. *Eur. J. Forest Res.* **123**, 259–267 (2004).
63. J. R. Williamson, W. A. Neilsen, The influence of forest site on rate and extent of soil compaction and profile disturbance of skid trails during ground-based harvesting. *Can. J. For. Res.* **30**, 1196–1205 (2000).
64. D. Hillel, "Surface runoff and water erosion" in *Introduction to Environmental Soil Physics*, D. Hillel, Ed. (Academic Press, 2003), pp. 283–295.
65. N. W. Shah *et al.*, The effects of forest management on water quality. *For. Ecol. Manage.* **522**, 120397 (2022).
66. K. D. Hannam, C. E. Prescott, Soluble organic nitrogen in forests and adjacent clearcuts in British Columbia. *Can. J. For. Res.* **33**, 1709–1718 (2003).
67. K. H. Venner, C. E. Prescott, C. M. Preston, Leaching of nitrogen and phenolics from wood waste and co-composts used for road rehabilitation. *J. Environ. Qual.* **38**, 281–290 (2009).
68. K. L. Clark, H. L. Gholz, M. S. Castro, Carbon dynamics along a chronosequence of slash pine plantations in north Florida. *Ecol. Appl.* **14**, 1154–1171 (2004).
69. J. Lehmann *et al.*, Persistence of soil organic carbon caused by functional complexity. *Nat. Geosci.* **13**, 529–534 (2020).
70. H. A. Mooney, E. E. Cleland, The evolutionary impact of invasive species. *Proc. Natl. Acad. Sci. U.S.A.* **98**, 5446–5451 (2001).
71. A. Hu *et al.*, Ecological networks of dissolved organic matter and microorganisms under global change. *Nat. Commun.* **13**, 3600 (2022).
72. USGCRP, 2018: "Second State of the Carbon Cycle Report (SOCCR2): A sustained assessment report," N. Cavallaro *et al.*, Eds. (U.S. Global Change Research Program, Washington, DC, 2018), p. 878.
73. J. E. C. Smyth *et al.*, "2023 blueprint for forest carbon science in Canada" (Natural Resources Canada, Canadian Forest Service, 2024).
74. R. Cristan *et al.*, Effectiveness of forestry best management practices in the United States: Literature review. *For. Ecol. Manage.* **360**, 133–151 (2016).
75. R. L. Beschta, W. L. Jackson, "Forest practices and sediment production in the Alsea Watershed study" in *Hydrological and Biological Responses to Forest Practices: The Alsea Watershed Study*, J. D. Stednick, Ed. (Springer New York, 2008), pp. 55–66.
76. K. R. Brown, W. Michael Aust, K. J. McGuire, Sediment delivery from bare and graveled forest road stream crossing approaches in the Virginia Piedmont. *For. Ecol. Manage.* **310**, 836–846 (2013).
77. I. K. Morrison, N. W. Foster, Fifteen-year change in forest floor organic and element content and cycling at the Turkey Lakes Watershed. *Ecosystems* **4**, 545–554 (2001).
78. I. K. Morrison, Organic matter and mineral distribution in an old-growth Acer saccharum forest near the northern limit of its range. *Can. J. For. Res.* **21**, 1153–1153 (1991).
79. N. W. Sokol *et al.*, Global distribution, formation and fate of mineral-associated soil organic matter under a changing climate: A trait-based perspective. *Funct. Ecol.* **36**, 1411–1429 (2022).
80. M. Lesiv *et al.*, Global forest management data for 2015 at a 100 m resolution. *Sci. Data* **119**, 1–14 (2022).
81. S. Linke *et al.*, Global hydro-environmental sub-basin and river reach characteristics at high spatial resolution. *Sci. Data* **6**, 283 (2019).
82. Y. Bergeron *et al.*, Projections of future forest age class structure under the influence of fire and harvesting: Implications for forest management in the boreal forest of eastern Canada. *Forestry* **90**, 485–495 (2017).
83. Natural Resources Canada, "The state of Canada's forests annual report" (Forestry Canada, 2022).
84. L. Peng, T. D. Searchinger, J. Zionts, R. Waite, The carbon costs of global wood harvests. *Nature* **620**, 110–115 (2023).
85. J. S. Rowe, *Forest Regions of Canada* (Information Canada, 1972).
86. K. L. Webster *et al.*, Turkey Lakes Watershed, Ontario, Canada: 40 years of interdisciplinary whole-ecosystem research. *Hydrol. Process.* **35**, e14109 (2021).
87. N. W. Foster, F. D. Beall, D. P. Kreutzweiser, The role of forests in regulating water: The Turkey Lakes Watershed case study. *For. Chron.* **81**, 142–148 (2005).
88. N. Foster, J. Spoelstra, P. Hazlett, S. Schiff, C. David, Heterogeneity in soil nitrogen within first-order forested catchments at the Turkey Lakes Watershed. *Can. J. For. Res.* **35**, 797–805 (2005).
89. G. Landry *et al.*, Mitigation potential of ecosystem-based forest management under climate change: A case study in the boreal-temperate forest ecotone. *For. Trees Livelihoods* **12**, 1667 (2021).
90. L. Boisvert-Marsh, C. Périé, S. de Blois, Shifting with climate? Evidence for recent changes in tree species distribution at high latitudes. *Ecosphere* **5**, 1–33 (2014).
91. D. S. Jeffries, J. R. M. Kelso, I. K. Morrison, Physical, chemical, and biological characteristics of the Turkey Lakes Watershed, central Ontario, Canada. *Can. J. Fish. Aquat. Sci.* **45**, s3–s13 (1988).
92. J. B. Lindsay, *Proceedings of the GIS Research UK 22nd Annual Conference* (The University of Glasgow, 2014).
93. J. F. O'Callaghan, D. M. Mark, The extraction of drainage networks from digital elevation data. *Comput. Vis. Graphics Image Process.* **28**, 323–344 (1984).
94. D. J. Pennock, B. J. Zebarth, E. De Jong, Landform classification and soil distribution in hummocky terrain, Saskatchewan, Canada. *Geoderma* **40**, 297–315 (1987).
95. A. J. Conacher, J. B. Dalrymple, The nine unit landsurface model: An approach to pedogeomorphic research. *Geoderma* **18**, 127–144 (1977).
96. C. D. Rennó *et al.*, Hand, a new terrain descriptor using SRTM-DEM: Mapping terra-firme rainforest environments in Amazonia. *Remote Sens. Environ.* **112**, 3469–3481 (2008).
97. A. D. Nobre *et al.*, Height above the nearest drainage–A hydrologically relevant new terrain model. *J. Hydrol.* **404**, 13–29 (2011).
98. OMNR, *Forest Management Guide for Conserving Biodiversity at the Stand and Site Scales* (Queen's Printer for Ontario, Toronto, 2010).
99. T. Dittmar, B. Koch, N. Hertkorn, G. Kattner, A simple and efficient method for the solid-phase extraction of dissolved organic matter (SPE-DOM) from seawater. *Limnol. Oceanogr. Methods* **6**, 230–235 (2008).
100. M. Pucher *et al.*, staRdom: Versatile software for analyzing spectroscopic data of dissolved organic matter in R. *Water* **11**, 2366 (2019).
101. A. R. Matteson, D. J. Mahoney, T. W. Gannon, M. L. Polizzotto, Integrated field lysimetry and porewater sampling for evaluation of chemical mobility in soils and established vegetation. *J. Vis. Exp.* **89**, 5182 (2014), 10.3791/51862.
102. A. Göttlein, U. Hell, R. Blasek, A system for microscale tensiometry and lysimetry. *Geoderma* **69**, 147–156 (1996).
103. J. Merder *et al.*, ICBM-OCEAN: Processing ultrahigh-resolution mass spectrometry data of complex molecular mixtures. *Anal. Chem.* **92**, 6832–6838 (2020).
104. F. W. McLafferty, F. Turecek, *Interpretation of Mass Spectra* (University Science Books, 1993).
105. D. E. LaRowe, P. Van Cappellen, Degradation of natural organic matter: A thermodynamic analysis. *Geochim. Cosmochim. Acta* **75**, 2030–2042 (2011).
106. B. P. Koch, T. Dittmar, M. Witt, G. Kattner, Fundamentals of molecular formula assignment to ultrahigh resolution mass data of natural organic matter. *Anal. Chem.* **79**, 1758–1763 (2007).
107. N. Hertkorn *et al.*, Characterization of a major refractory component of marine dissolved organic matter. *Geochim. Cosmochim. Acta* **70**, 2990–3010 (2006).
108. A. M. Kellerman, T. Dittmar, D. N. Kothawala, L. J. Tranvik, Chemodiversity of dissolved organic matter in lakes driven by climate and hydrology. *Nat. Commun.* **5**, 3804 (2014).
109. J. M. Chase, N. J. B. Kraft, K. G. Smith, M. Vellend, B. D. Inouye, Using null models to disentangle variation in community dissimilarity from variation in α-diversity. *Ecosphere* **2**, art24 (2011).
110. W. Kew *et al.*, Reviews and syntheses: Opportunities for robust use of peak intensities from high-resolution mass spectrometry in organic matter studies. *Biogeosciences* **21**, 4665–4679 (2024).
111. F. D. Beall, R. G. Semkin, D. S. Jeffries, Trends in the output of first-order basins at Turkey Lakes Watershed, 1982–96. *Ecosystems* **4**, 514–526 (2001).
112. I. K. Morrison, G. D. Hogan, Trace element distribution within the tree phytomass and forest floor of a tolerant hardwood stand, Algoma. *Water Air Soil Pollut.* **31**, 493–500 (1986).
113. S. H. Lamlom, R. A. Savidge, Carbon content variation in boles of mature sugar maple and giant sequoia. *Tree Physiol.* **26**, 459–468 (2006).
114. H. S. Wauchope *et al.*, Evaluating impact using time-series data. *Trends Ecol. Evol.* **36**, 196–205 (2021).
115. J. Pinheiro, D. Bates, R Core Team, nlme: Linear and nonlinear mixed effects models. (2023). R package version 3.1-163. https://CRAN.R-project.org/package=nlme. Accessed 10 February 2023.
116. R Core Team, *R: A Language and Environment for Statistical Computing* (R Foundation for Statistical Computing, Vienna, Austria, 2021).
117. M. E. Brooks *et al.*, glmmTMB balances speed and flexibility among packages for zero-inflated generalized linear mixed modeling. *R J.* **9**, 378–400 (2017).
118. E. C. Freeman, E. Emilson, K. Webster, T. Dittmar, A. Tanentzap, PNAS: Logging disrupts the ecology of molecules in headwater streams (v1.0.1). Zenodo. https://doi.org/10.5281/zenodo.16677581. Deposited 1 August 2025.